The Proceedings of the International Conference on Creationism

Volume 8
Print Reference: Pages 673-682

Article 15

2018

Modeling of Flood and Post-Flood Ocean Floor Cooling

William J. Worraker
Biblical Creation Trust

Richard Ward
Biblical Creation Trust

Worraker, W.J., and R. Ward. 2018. Modeling of Flood and post-Flood ocean floor cooling. In *Proceedings of the Eighth International Conference on Creationism*, ed. J.H. Whitmore, pp. 673–682. Pittsburgh, Pennsylvania: Creation Science Fellowship.

MODELING OF FLOOD AND POST-FLOOD OCEAN FLOOR COOLING

William J. Worraker, Biblical Creation Trust, P.O. Box 325, Ely, CB7 5YH, United Kingdom, wworraker@gmail.com
Richard Ward, Biblical Creation Trust, P.O. Box 325, Ely, CB7 5YH, United Kingdom, richard.ward@cantab.net

ABSTRACT

Given that the earth's ocean basins are geologically young, few areas being older than early Jurassic, and that most creation scientists regard Jurassic rocks as Flood deposits, these basins must have formed during and since the Flood, i.e. within no more than 4500 years. This paper represents a first attempt at modeling ocean basin formation by the separation of the continents and cooling of mantle material emplaced at spreading centres well within that limited time. We use a spreadsheet-based finite difference solution of the heat diffusion equation applied to a simple widely-used plate model of ocean lithosphere formation. Having verified our model by reproducing in detail the results of published uniformitarian calculations, we use it to demonstrate the effects of enhanced heat conduction and of a variety of heat sinks, both uniform and tailored in space and time, within a biblical time scale. Enhanced heat conduction is physically unrealistic and delivers an overwhelming heat load to the oceans, thus requiring two extraordinary changes to normal physics. A tailored heat sink reproduces surface heat flux and bathymetry profiles of the observed general forms, but predicted heat fluxes in the broad near-ridge region are far too high, and ridge profiles are too sharp. These problems stem from the presence of an apparently unavoidable near-surface thermal boundary layer. Including more realistic initial conditions and taking account of hitherto neglected geophysical processes (e.g. phase changes during magma depressurization, water production and fluid convection) to construct more sophisticated models are suggested as possible ways forward from this impasse.

KEY WORDS

Ocean floor; Jurassic; lithosphere; conduction; heat flow; spreading rate; modeling

INTRODUCTION

Today's ocean floors are geologically young, few areas being older than early Jurassic. In uniformitarian terms this is about 200 million years old at most (Müller et al. 2008). Oceanic lithosphere consists mainly of cooling mantle material emplaced at mid-ocean ridges and spreading centres, with an overlying layer of sediment. Most of this sediment is less than 5 km thick over the larger central parts of the Atlantic and Pacific oceans (Whittaker et al. 2013). In thermal modeling oceanic lithosphere is typically taken to be about 100 km thick, although its bottom boundary is not precisely defined (McKenzie et al. 2005, Crosby et al. 2006). Both sediment and lithosphere thicken progressively away from spreading centres. Ocean tectonic plates are currently moving at half spreading rates of a few centimetres per year, e.g. ~2 cm/year in the North Atlantic, ~10 cm/year around the East Pacific Rise (Müller et al. 2008). Although these present day rates are based on data such as GPS and space geodesy measurements, accepted plate tectonic histories of ocean basins are deduced mainly from the uniformitarian ages of magnetic anomaly patterns (Müller et al. 2008, Seton et al. 2012).

The total upward heat flow into the oceans is 32 TW (terawatts), which implies an average oceanic heat flux of 105 mWm^{-2} (milliwatts per square metre; see Davies and Davies 2010). The minimum heat flux (for the oldest ocean floor) is approximately 48 mWm^{-2} (Stein and Stein 1992), while the maximum, which occurs at mid-ocean ridges, is approximately 450 mWm^{-2} (Davies and Davies 2010); even higher heat fluxes may occur at volcanic hot-spots, but these cannot be accounted for in the global average models considered here. However the above figures serve as observational checks against our model predictions.

Given that most creation scientists regard Jurassic rocks as Flood deposits, the ocean basins must have formed during and since the Flood, and most oceanic lithosphere must have cooled to its present state within that time, i.e. in no more than 4500 years, probably far less. Considerable heat is deposited by the material surfacing at spreading centres: Furlong and Chapman (2013) estimate a total heat load of ~3.9×10^{14} joules per square metre of fresh ocean lithosphere, more than 30 times enough to boil off the oceans if deposited very rapidly. The associated "heat problem" is to determine how the cooling was accomplished in a short time (Barnes 1980), given that sea-floor climate proxies (notably oxygen-18 levels in marine fossil shells, quoted as $\delta^{18}O$ values) do not exhibit high-temperature excursions above about 12°C as seen in the Paleocene-Eocene Thermal Maximum (Zachos et al. 2001, Cramer et al. 2009, Mudelsee et al. 2014).

The approach taken here is to undertake a spreadsheet analysis of a plate cooling model based on those considered by Parsons and Sclater (1977) and by Stein and Stein (1992). Although plate models embody a drastic simplification of the physics of lithosphere formation by cooling (Crosby et al. 2006), they have been widely used and for many purposes give useful results for comparison with field data. Furthermore, since we are considering time scales several orders of magnitude shorter than those assumed in the secular literature, secondary effects such as near-surface hydrothermal cooling, latent heat effects related to partial melting of magma, or nonuniform convective motion in the underlying mantle, can justifiably be neglected in the first instance.

We first analyse the model of Stein and Stein (1992) on the assumption of uniformitarian time scales in order to verify by comparison with their results that our spreadsheet is correctly set up. We then consider variations on our basic model involving (1) extremely high thermal conductivity, and (2) various spatial

Table 1. Model parameter values used by Stein and Stein (1992) in their GDH1 model and in the baseline model employed here. PSM refers to the values used by Parsons and Sclater (1977). The figures prefixed by ± are the 1σ uncertainty margins estimated by the respective authors.

Parameter	Symbol	Value	Units	Notes
Plate thickness	L	95(±15)	km	PSM: 125(±10)
Basal temperature	T_1	1450(±250)	ºC	PSM: 1350(±275)
Coefficient of thermal expansion	α	$3.1(\pm0.8)\times10^{-5}$	K^{-1}	PSM: $3.2(\pm1.1)\times10^{-5}$
Specific heat	C_p	1171	$J\ kg^{-1}\ K^{-1}$	
Thermal Conductivity	k	3.138	$W\ m^{-1}\ K^{-1}$	
Mantle density	ρ_m	3330	$kg\ m^{-3}$	
Water density	ρ_w	1000	$kg\ m^{-3}$	
Ridge depth	d_R	2.6	km	PSM: 2.5

and temporal forms of artificial heat sink, in order to investigate possible ways of achieving the necessary cooling within biblical time scales. Accelerated plate motion defines the relationship between time and distance from the spreading centre in these cases; without this the predicted bathymetry would be hopelessly at odds with real ocean floor bathymetry. In this connection we note that in developing models of Catastrophic Plate Tectonics (or CPT, Austin et al. 1994), Baumgardner (2003) predicts maximum plate speeds measured in metres per second, about 9-10 orders of magnitude faster than present-day values. In this paper we ignore the possible impact of accelerated nuclear decay in order to address in isolation the problem of generating the earth's oceanic lithosphere by cooling within the post-Flood period.

The key observables from each modeling exercise are plate vertical shrinkage (manifested as bathymetry) and surface heat flow. Comparison of these with global field data then reveals whether the models we are analysing stand any chance of explaining, even at the crudest level, how ocean lithosphere could have formed in a short time. Even at the outset we make no claim to be able to solve the post-Flood ocean floor heat problem, nor to determine whether supernatural intervention is needed. Rather, we seek to define the key characteristics of cooling processes which could have produced today's ocean floor bathymetry and heat flows within a biblically compatible time scale.

In the following sections we describe the modeling procedure – model structure and parameters, and the physical processes represented in our models. We then describe the methods of solution, the issues raised by the presence of a thermal boundary layer, and the inclusion of plate motion. Our results are described in four sections – the uniformitarian case, accelerated thermal conduction, a uniform heat sink and a tailored heat sink. We then discuss specific issues arising from our results, viz. the enhanced thermal conduction hypothesis, the impact of the initial conditions, the role of the thermal boundary layer and suggestions for further work. This is followed by our conclusion.

MODEL DESCRIPTION

1. Physical Parameters

Our reference model, including the necessary physical parameter values, is that of Stein and Stein (1992), referred to as GDH1 (for global depth and heat flow). This is based on the earlier work of Parsons and Sclater (1977), whose main plate model is known as PSM. Stein and Stein used a much larger database than Parsons and Sclater and considered the effect of varying a number of input parameters used by Parsons and Sclater in order to optimize the fit of their model results to the available ocean floor heat flow and bathymetry data from the North Pacific and Northwest Atlantic; GDH1 is intended as a global reference model. The parameter values chosen by Stein and Stein, and also used here, are given in Table 1, which also includes their estimated margins of uncertainty. Although in reality the thermal conductivity and thermal expansion coefficient of the cooling lithosphere depend on temperature and pressure, for simplicity these are treated as constant both here and in the literature. The temperature at the surface is implicitly fixed at 0ºC.

2. Physical Processes

The fundamental process modelled here is the conduction of heat through the bulk of the cooling lithosphere, into it at the base and out of it at the surface. Because of motion away from the spreading centre (mid-ocean ridge), the governing equation of energy flow includes both convective and diffusive terms. In practice temperature gradients in the spreading direction are much smaller than in the vertical direction such that horizontal heat flow, both convective and diffusive, can safely be neglected. The equation to be solved thus reduces to the one-dimensional time-dependent heat diffusion equation, viz.

$$\frac{\partial T}{\partial t} = \kappa \frac{\partial^2 T}{\partial z^2} \qquad (1)$$

where T is temperature, t time, κ thermal diffusivity ($\equiv k/\rho C_p$), and z distance below the surface. The boundary conditions for plate models are fixed temperature, viz. $T=T_0$ at $z=0$ and $T=T_1$ at $z=L$, where L is the plate thickness. The initial condition is $T=T_1$ everywhere except at $z=0$; this introduces a singularity in the solution at $z=0$, $t=0$. This does not cause any significant problems in the solution procedure for the long time scale model. For the short time scale calculations it does introduce problems related to mesh resolution and the occurrence of a near-surface thermal boundary layer; these are considered in the 'Methods of solution' section (part 3), the 'Results' section (part 4) and the 'Discussion' section (part 3).

Because of the above decoupling of the heat diffusion process from the outward material motion, the solution to equation (1) at any

given time is effectively transported outward from the spreading centre at the same rate as the lithospheric material. In the secular literature the model data (temperature profiles, heat fluxes and shrinkage) are plotted against geological time; distance per se is ignored. This is consistent with the use of these models as global reference models, to be compared with globally averaged data, given that plate spreading speeds vary considerably between ocean basins. Thus, for example, near the East Pacific Rise current spreading rates are much higher (~10 cm/year) than in the North Atlantic (~2 cm/year; Müller et al. 2008), and mid-ocean ridges are correspondingly wider in the East Pacific Rise. For our short time scale calculations, we treat the spreading rate as a free parameter, to which we assign a predefined profile in time. This in turn enables us to define the resulting bathymetry in terms of calculated shrinkage against distance.

The vertical shrinking of the cooling lithosphere is essentially thermal contraction and is therefore calculated from the total net heat loss. However the surface depression is greater than would be calculated simply from the heat lost by a column of lithosphere. This is because the water loading increases as the lithosphere shrinks and becomes denser, and the water depth increases. In turn this is isostatically compensated by further depression of the ocean floor (for a derivation see Turcotte and Schubert 2002, section 4.23). Thus for lithospheric density ρ_m and water density ρ_w, there is a shrinkage enhancement factor $\gamma \equiv \rho_m/(\rho_m-\rho_w)$, such that the total shrinkage for a column of height L when the average temperature has fallen from T_1 to T_m is given by

$$\delta z = \gamma \alpha L(T_m - T_1). \qquad (2)$$

For the data values given in Table 1, the enhancement factor is $\gamma = 1.429$.

METHODS OF SOLUTION

1. Analytical solution

The earliest and simplest model used to analyse ocean floor cooling is known as the infinite half space model (Turcotte and Schubert 2002, section 4.15), which has an analytical solution in terms of error functions. For surface temperature T_0 and deep-mantle temperature T_1, this gives a heat flux to the ocean at time t of

$$q(t) = \frac{k(T_1 - T_0)}{\sqrt{\pi \kappa t}}. \qquad (3)$$

Integrating this expression with respect to time then gives the total heat lost (expressed in joules per square metre) to the ocean as

$$Q(t) = \frac{2k(T_1 - T_0)}{\sqrt{\pi \kappa}} t^{1/2}. \qquad (4)$$

Given that the heat loss for a finite-thickness plate can be expressed in the form

$$Q = \rho C_p L(T_1 - T_m), \qquad (5)$$

comparison of equation (4) with (2) implies that for the half space model the net shrinkage is

$$\delta z = \frac{\gamma \alpha}{\rho C_p} \frac{2k(T_1 - T_0)}{\sqrt{\pi \kappa}} t^{1/2}. \qquad (6)$$

Parsons and Sclater (1977), in comparing the predictions of the half space model with bathymetry data, conclude that the model gives a good approximation to reality up to about 70 Ma in the conventional time frame. Beyond this it overpredicts the surface depression due to shrinkage, which indicates that shrinkage is limited by heat transfer from the underlying mantle into the lithosphere. This behaviour (a $t^{½}$ dependence of the bathymetry up to a limited time) was also seen in previous plate models; Parsons and Sclater's plate model parameters were chosen to optimize the data fit up to about 160 Ma. Stein and Stein (1992) improved the fit with a much larger dataset and formal procedures for optimizing their input parameters. In both of these papers the solution of the heat diffusion equation was obtained analytically in terms of infinite Fourier series in z, the terms decreasing exponentially in x (distance from the ridge). Because of computational difficulties in evaluating such series, here we use a simple finite difference timestepping scheme which can readily be evaluated on an Excel© spreadsheet. For reference purposes Stein and Stein give approximate fitting equations based on their GDH1 model for surface heat flux and ocean depth against uniformitarian time. Their heat flux equation for time $t \leq 55$ Ma (million years) is

$$q(t) = 0.510t^{-1/2} \qquad (7)$$

and for $t > 55$ Ma,

$$q(t) = 0.048 + 0.096e^{-0.0278t} \qquad (8)$$

where t is measured in Ma and $q(t)$ in Wm^{-2}. Their depth equation for $t < 20$ Ma is

$$d(t) = 2.6 + 0.365t^{1/2} \qquad (9)$$

and for $t \geq 20$ Ma,

$$d(t) = 5.651 - 2.473e^{-0.0278t} \qquad (10)$$

where $d(t)$ is measured in km and t again in Ma. We use these later as comparisons for the results of our spreadsheet modeling exercise.

2. Finite difference solution

The heat diffusion equation belongs to the class of second-order partial differential equations (PDEs) designated *parabolic*. The simplest widely-used scheme for solving the finite difference equations generated by discretization of parabolic PDEs is the *classic explicit* method (Lapidus and Pinder 1982). Applied to the one-dimensional time-dependent heat diffusion equation, the term *explicit* here means that the temperature at any given point in space is updated in a timestep directly from local temperatures at the start of the timestep. By contrast *implicit* methods involve multiple temperatures at both beginning and end of the timestep, and updating a temperature value may involve iteration or matrix inversion. Thus explicit methods are simpler to set up and computationally faster than implicit methods, but tend to become unstable – the solution becoming wildly ridiculous – more readily than with implicit methods.

We employ uniform discretization in both t and z, such that the temperature at each point in time and space has two suffixes, i.e. $T_{i,j}$ where i (=0, 1, 2 . . .) denotes the point in time and j (=0, 1, . . . n) the point in space, where i=0 refers to initial conditions (t=0), j=0 to the surface (z=0) and j=n to the plate bottom (z=L). In the classic

explicit method $T_{i,j}$ is thus updated as follows:

$$T_{i+1,j} = T_{i,j} + \mu\left(T_{i,j-1} - 2T_{i,j} + T_{i,j+1}\right). \qquad (11)$$

where $\mu \equiv \kappa\Delta t/(\Delta z)^2$, a parameter which serves as a dimensionless timestep; Δt is the actual timestep and Δz the mesh spacing. Equation (11) is based on a locally quadratic approximation to the temperature field. Thus the (upward) surface heat flux, where j=0, is given by

$$q_{i,0} = k\left[\left(T_{i,1} - T_{i,0}\right) - \frac{1}{2}\left(T_{i,2} + T_{i,0} - 2T_{i,1}\right)\right]/\Delta z \qquad (12).$$

Stability of this scheme requires that $\mu \leq 0.5$ (Lapidus and Pinder 1982, section 4.4). For the scheme to produce a solution corresponding to the solution of the original heat diffusion equation, the key property of *convergence*, the original PDE (including boundary and initial conditions) must be well-posed, the difference equation (11) must be consistent with it, and the scheme must be stable. This further implies the necessity for *mesh convergence*, i.e. as the mesh is refined in both t and z directions, the solution must tend to a final form.

In cases involving a heat sink characterized by a function $h(z, t)$, the fundamental heat diffusion equation (1) becomes

$$\frac{\partial T}{\partial t} = \kappa\frac{\partial^2 T}{\partial z^2} - \frac{h(z,t)}{\rho C_p} \qquad (13)$$

where in our spreadsheets $h(z, t)$ is given in units of Wm^{-3} (watts per cubic metre), ρ is density in kgm^{-3} and C_p is specific heat capacity in $Jkg^{-1}K^{-1}$. In practice, the final form of heat sink is made proportional to the difference between the temperature at a point within the plate and the temperature there with the system in thermal equilibrium. The difference equation (11) thus becomes

$$T_{i+1,j} = T_{i,j} + \mu\left(T_{i,j-1} - 2T_{i,j} + T_{i,j+1}\right) - \frac{\Delta t}{\tau_{hs}}\left\{T_{i,j} - [T_0 + z(T_1 - T_0)/L]\right\} \qquad (14)$$

where τ_{hs} is our choice of heat sink lifetime. The inclusion of a heat sink in the difference equation means that the analysis underlying the stability criterion $\mu \leq 0.5$ given by Lapidus and Pinder (1982) no longer applies. However where we have included a heat sink the timestep is very small ($\mu < 10^{-5}$) and we can use observed mesh convergence to strengthen confidence that our calculations in these cases are essentially correct and stable in that no result depends critically on the timestep and mesh size.

Equations (11) and (14) are readily implemented in our spreadsheets, together with the fixed temperature boundary conditions at the top and bottom of the plate and the initial condition simply as the first column of $T_{i,j}$ values with i=0 and j=0, 1, . . .n. (i.e. $T_{i=0,j=0}=T_0$, $T_{i=0,j=1,2,\ldots n}=T_1$). The total heat loss is calculated using equation (5), where T_m is the average of all the mid-interval temperatures through the lithospheric column, and then the shrinkage from equation (2). However calculation of the surface heat flux is complicated by the existence of a thermal boundary layer near the surface and associated mesh resolution issues. These are considered in the following subsection.

3. The thermal boundary layer and mesh resolution

In mathematical terms a boundary layer is a narrow region where the solution of a differential equation changes rapidly. It occurs when the highest-order term in the equation is multiplied by a small parameter $\varepsilon << 1$ and must have the property that the layer thickness $\delta \to 0$ as $\varepsilon \to 0$ (Bender and Orszag 1978). Here in physical terms we are dealing with the downward propagation of a broadening cooling front from the surface of initially hot material subject to the heat diffusion equation (1). At relatively early times, when the cooling front has only propagated a short distance downwards such that it has not yet felt the influence of the bottom boundary, the solution of the half space model is a good approximation to the cooling process. In this case the temperature field depends only on the combination $\eta \equiv z/2\sqrt{\kappa t}$, and after time t the cooling front will have propagated a distance of order $\sqrt{\kappa t}$. This propagation distance defines a thermal boundary layer whose thickness may be formalized as $\delta_{th} \equiv \sqrt{\pi\kappa t}$ such that equation (3) for the surface heat flux in the half space model may be written in the form $q(t) = k(T_1 - T_0)/\delta_{th}$.

If the timestep Δt is much smaller than the stability limit, i.e., $\mu << 0.5$, as is the case in our short time scale calculations with κ retaining its natural value ($\approx 8\times10^{-7}$ m^2/s), there will be a thin thermal boundary layer, defined by $\delta_{th} << \Delta z$ for some time. In these cases the surface heat flux, shrinkage and temperatures through the column of lithosphere are best calculated from the half space model because the spatial discretization is too coarse to resolve the near-surface temperature variation. However this is only possible in the absence of a heat sink since the half space model solution is no longer valid if there is a heat sink in operation.

In the long time scale calculation, with Δz = 950 m and Δt = 10,000 years, the boundary layer thickness after a single timestep is 893 m, which is comparable with Δz. However close to the surface the heat flux and temperature variation are not well approximated locally by a quadratic form; equations (11) and (12) still give inaccurate results. In these circumstances the results for the half space model are used instead until after a few hundred timesteps, when the mesh resolution has become adequate and the now very broad cooling front is just about to interact noticeably with the bottom boundary. In our model this switch-over point, although somewhat arbitrary, is taken to be at 8.0 Ma.

In the above cases where mesh resolution and the curvature of the temperature profile render the discretized calculation inaccurate, special care has to be taken in the calculation of total heat loss and consequently of shrinkage. In principle the total heat loss is calculated from the sum of heat losses for individual z intervals, which depend on the drop in average temperature for each. The simplest way of calculating this sum is by the *trapezoidal rule*, which treats the temperature variation between mesh points as linear. For cases with a significantly curved temperature profile we employ *Simpson's rule* instead; this is based on a piecewise quadratic approximation to the temperature profile, and for the most extreme points (i.e. adjacent to the plate surface in the first few timesteps) gives an order of magnitude improvement in the accuracy of the result. It is not needed beyond the switch-over

point as the trapezoidal rule is then perfectly adequate.

4. Spreading rate

In the long time scale calculations we treat the spreading rate as a constant, a rough equivalent of the present-day half spreading rate for the Atlantic, i.e. 2.5 cm/year. Although uniformitarian authors use the accepted timings of magnetic field reversal markers to infer ocean basin spreading histories without the assumption of constant spreading rates, the above fixed rate is sufficient for the purpose of comparing our spreadsheet results with their published model predictions.

Given our assumption that the present-day ocean floors have in reality formed during and since the Flood, they must have spread several thousand kilometres in no more than 4500 years, implying an average half spreading rate of order 0.5-1 km/year. Furthermore Baumgardner's (2003) 3D model of CPT implies maximum plate speeds measured in metres per second. Thus there must have been a brief phase of rapid plate motion which is most naturally associated with the Flood and its immediate aftermath. Baumgardner's simulations naturally suggest that the motion quickly accelerated to a maximum near the onset of the Flood and then subsided continuously down to present-day rates. However our simulations only seek to model the latter part of the Flood and the following 4400 years. Assuming that the Flood produced the rocks conventionally dated between 600 Ma and 65 Ma (Vardiman et al. 2005), and that today's ocean floors date from 200 Ma, we are covering only (200-65)/(600-65) ≈ 0.25 of the Flood, together with the post-Flood period. The simplest way to model this is to assume a constant high spreading rate for 0.25 year, which then decays exponentially to present-day rates. Thus in the final form of our spreadsheet models we use a half spreading rate of the form

$$v(t) = v_p + v_0\,, t \le \tau_f \qquad (15a)$$

$$v(t) = v_p + v_0 \exp\left(-\frac{t-\tau_f}{\tau_d}\right), t > \tau_f \qquad (15b)$$

where υ_ρ is the present-day half spreading rate, υ_0 is a reference half spreading rate, τ_f is the Flood period covered in the simulation, and τ_d is the characteristic decay time of the plate motion. The maximum half spreading rate is thus $\upsilon_p + \upsilon_0$. The values of υ_0, τ_f and τ_d are not independent because the total distance travelled since Flood onset, $\approx \upsilon_0(\tau_f + \tau_d)$, must amount to a few thousand km. For values of υ_0 in the range expected (of order 0.1-1 ms^{-1}) this constrains τ_d to a value of order 1 year or less. We thus assume rapid post-Flood decay of plate motion and set τ_d = 0.2 year.

The ratio τ_{hs}/τ_f (see equations 14 and 15) determines the shape of the heat flux and depth profiles against distance from the ridge axis, and hence their variation against equivalent uniformitarian time.

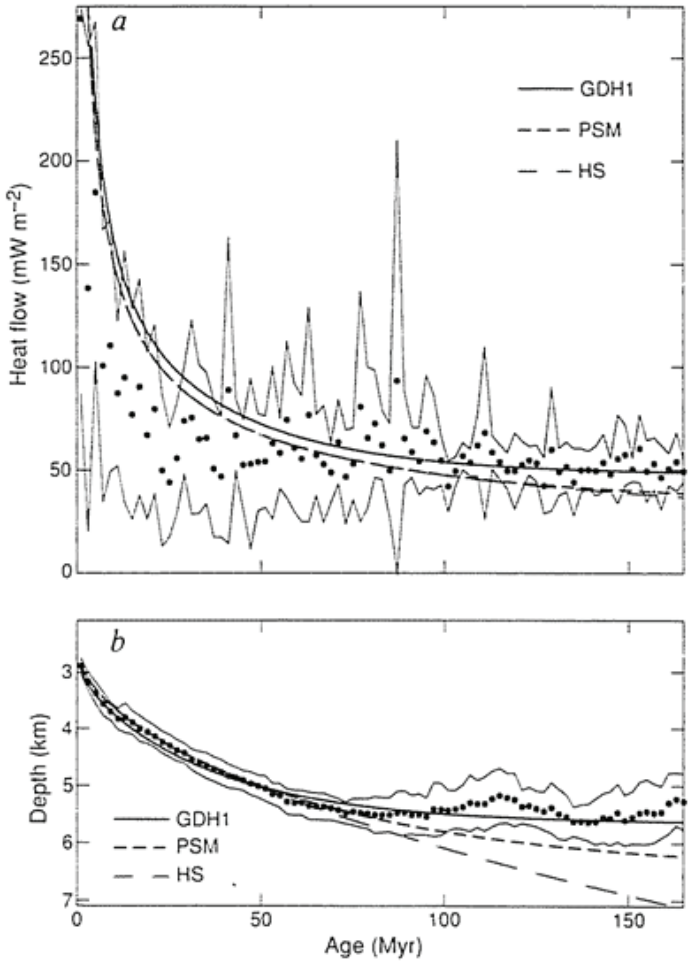

Figure 1. Fig. 1 from Stein and Stein (1992), showing the comparison of the half space model (HS), Parsons and Sclater's (1977) plate model (PSM) and their own GDH1 plate model against global average data. The assumed ridge depth here is 2.5 km. The data (shown by dots) are averaged in 2 Ma bins and the envelopes (wavy/spiky lines) delineate one standard deviation about the mean.

RESULTS

1. Repeat of uniformitarian calculation

The uniformitarian or long time scale calculation aimed at verifying that our spreadsheet is correctly set up is done on a mesh with 100 intervals along the vertical axis of Δz = 950 metres each, the timestep being Δt = 10,000 years. Given the input parameters in Table 1, these intervals correspond to a dimensionless timestep μ = 0.2841, well within the stability limit. The calculation is continued up to a simulated time of 200 Ma.

Stein and Stein's (1992) predictions for surface heat flux and ocean depth up to 160 Ma are reproduced in Fig. 1 here. Note that their model overpredicts heat fluxes close to spreading centres, as also do the half space and PSM models. This is generally attributed to the effect of heat transport by hydrothermal flows in young lithosphere with very little sediment cover (Stein and Stein 1992, Qiuming 2016). The data also show a decrease in depth in the 90-130 Ma range of uniformitarian ages, which is not predicted by these models; this has been attributed to mantle convection (Crosby et al. 2006).

Our results for the equivalent case are shown in Figs. 2 and 3. It is clear that our spreadsheet-based predictions are extremely close to those of Stein and Stein's (1992) GDH1 model; the visible difference in predicted depth at large times, notably for the half space model at 150 Ma, arises because the ridge depth in Stein and Stein's (1992) Fig. 1 is 2.5 km [they have used Parsons and Sclater's (1977) value for comparison]; here we have used their preferred value of 2.6 km. Our figures for final values of heat flux and depth match theirs as closely as can be judged. Plots of the temperature profile at various times in our calculation are shown in Fig. 4; by 200 Ma simulated time conditions have almost reached steady state. Exactly as in Stein and Stein's (1992) GDH1 model, our model overpredicts heat fluxes close to spreading centres and does not predict the shallowing observed in older ocean

lithosphere. However it does reproduce Stein and Stein's results by an alternative numerical method, which demonstrates the success of our verification exercise.

As a verification of mesh convergence in our calculations we have repeated them on another spreadsheet with finer discretization, viz. Δz = 475 m and Δt = 2,500 years; to preserve the same μ value halving Δz requires a 4 times smaller value of Δt . This calculation is continued to a simulated time of 10 Ma. The only differences visible in the spreadsheets at 10 Ma are in the heat fluxes, being of order 1 in the fourth significant figure for the surface heat flux and 4 in the second significant figure in the bottom heat flux; since the latter is very small (~10^{-5} Wm^{-2}), these differences are insignificant.

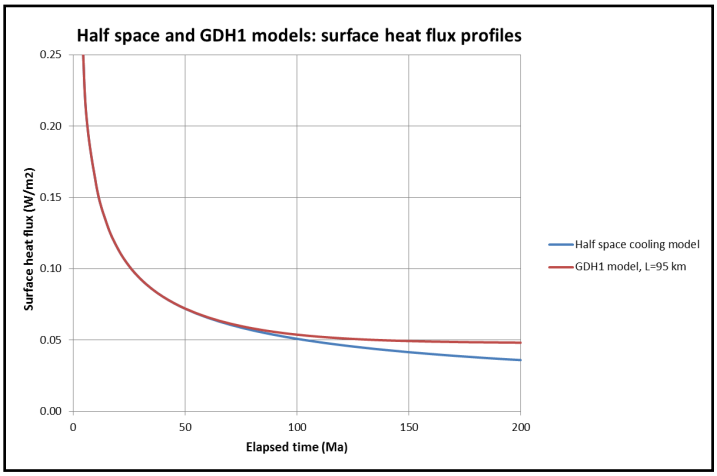

Figure 2. Plot of the surface heat flux for the half space model and the GDH1 model of Stein and Stein (1992), taken from our spreadsheet calculations with Δz = 950 metres and Δt = 10^4 years such that the dimensionless timestep μ=0.2841. By construction the curves are identical up to t=8.0 Ma. The results are graphically indistinguishable from those presented in Stein and Stein's (1992) Fig. 1a. Given the considerable scatter on the data points in their plot, the GDH1 model becomes distinguishable from the half space model at about 120 Ma.

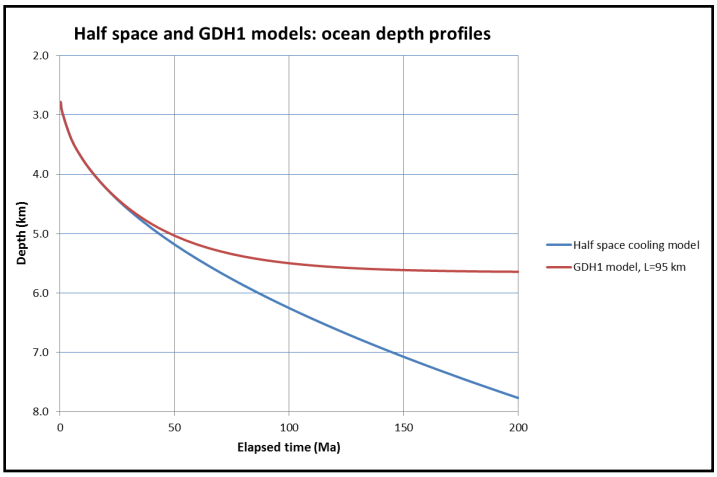

Figure 3. Plot of the ocean depth profiles for the half space model and the GDH1 model of Stein and Stein (1992), taken from our spreadsheet calculations with the same mesh size and timestep as in Fig. 1. These model plots are practically the same as those in Stein and Stein's Fig. 1b, and it is clear that the models give divergent results at an earlier time for ocean depth than for surface heat flux. The curves are slightly lower here compared with those in Fig. 1 because the ridge depth there was 2.5 km vs. 2.6 km here.

2. Accelerated heat conduction

The half space and GDH1 model calculations were repeated with drastically higher thermal conductivity and correspondingly shorter timesteps in order to show the effect of seeking to cool the lithosphere in a biblically-compatible time scale simply by accelerating the heat conduction process. Thermal conductivity is increased by a purely illustrative factor 10^9, while the timestep is reduced by the same factor. To maintain the same ocean floor profile the uniform spreading rate is also accelerated by a factor of 10^9. Given that the computational mesh is kept as before (Δz = 950 m), this means that the combination $\kappa\Delta t$ and hence μ are also the same. Not surprisingly, therefore, the temperature field and shrinkage are identical to those obtained in the uniformitarian case, while surface heat fluxes are 10^9 times larger than before at corresponding points in time; however the total simulated time is now only 0.2 of a year (about 73 days) instead of 200 million years. Thus the total surface heat load of 4.58×10^{14} Jm^{-2} is deposited into the above-surface environment in only 73 days, an average surface heat flux exceeding 70 MWm^{-2} (The net heat loss, which gives rise to the vertical shrinkage, is only 2.68×10^{14} Jm^{-2}, the difference being accounted for by heat transfer into the plate from the hotter region below).

The above high rate of heat loss could not be sustained naturally by the earth's oceans. Since even blackbody radiation from a free surface at 1,450ºC can only remove 500 kWm^{-2}, this enhanced conduction scenario demands an extraordinary surface cooling mechanism in addition to the postulated extraordinarily efficient heat conduction within the cooling lithosphere. The "enhanced thermal conduction hypothesis" is considered further in the discussion section below.

3. A uniform heat sink

The attraction of postulating an internal heat sink to cool the lithosphere is that the above-surface environment is only subject to modest heat loads; it does not necessarily "know" about exceptional sub-surface processes. Furthermore there have been suggestions in the creation science literature of an expansion of space during the Flood as a way of providing volume cooling (see Humphreys 2000, pp.369-374, and Humphreys 2005, pp.67-74); in models of the kind investigated here such a process would be manifested as a heat sink. We therefore repeat the calculations of the previous section

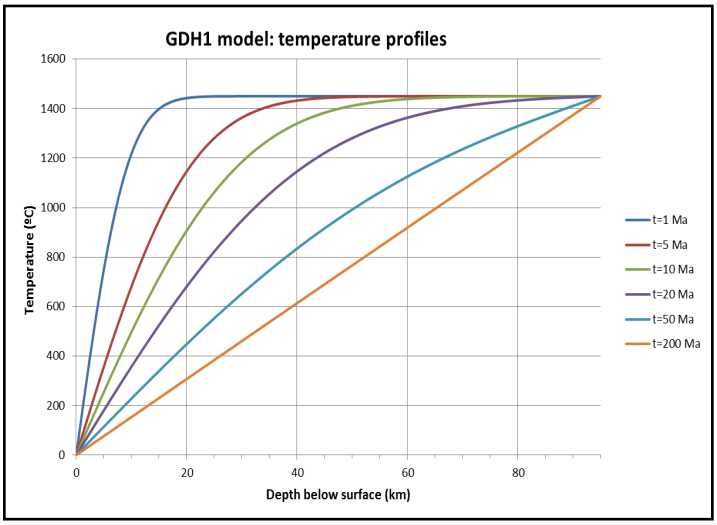

Figure 4. Temperature profiles through the depth of the plate from our spreadsheet calculations of the GDH1 model (Stein and Stein 1992). Note that by 200 Ma the profile is practically straight – by this time the system has almost reached its asymptotic steady state condition.

with a normal value of thermal conductivity but with a uniform heat sink over a specified time. We have chosen an illustrative heat sink lifetime of 0.2 year (73 days), of a magnitude chosen to remove the same amount of heat as would be lost in total if the lithosphere cooled naturally down to steady state conditions. The spreading rate is taken as constant through this interval at 0.63 ms^{-1}, which is 10^9 times faster than present-day rates. The predicted surface heat flux after 73 days is 570 Wm^{-2}, falling to 3.8 Wm^{-2} after a further 4400 years to account for the post-Flood period.

Figs. 5 and 6 show that, although the total heat loss in the GDH1 model is the same as in the long time scale calculation, most of it (>99.99%) is swallowed by the heat sink. In this case the predicted surface heat flux is much higher than in the long time scale calculation; even today it would be over 40 times higher than observed, and the depth profile is linear. Both predictions are contrary to observation. The depth profile could be modified by a different time dependence of the spreading rate, viz. by accelerating from a slow start, but this would not improve the surface heat flux prediction.

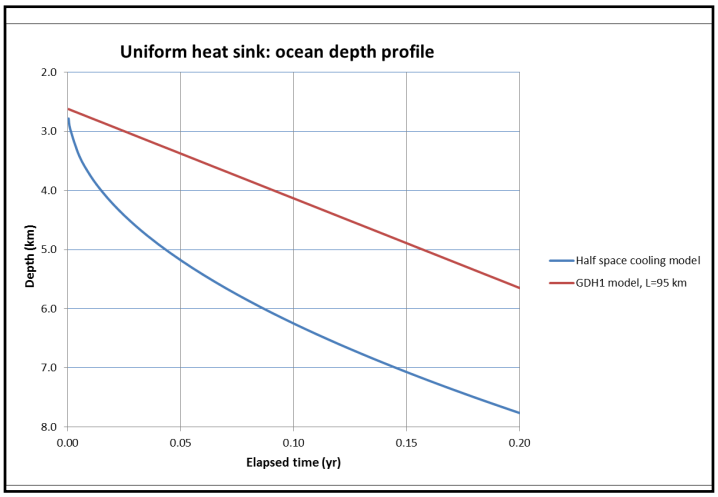

Figure 5. Plot of ocean depth profile in the case of a uniform heat sink lasting for 0.2 years (73 days). In this case the GDH1 model shows a linear profile because almost all of the plate's heat loss is due to the heat sink. The thermal conductivity value used here in the half space model is 10^9 times larger than its natural value in order to match the depth profile seen in Fig. 3 over the relevant (now very short) life of the heat sink.

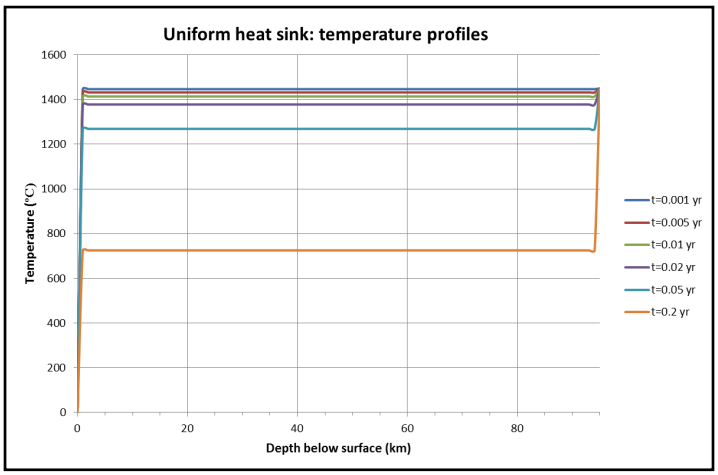

Figure 6. Temperature profiles in the GDH1 model with a uniform heat sink lasting for 0.2 years (73 days). These are essentially flat except in thin thermal boundary layers near the top and bottom of the plate. Consequently the heat flux at the surface is much higher than in the long time scale calculation, but overall most of the heat loss (>99.99%) is due to the heat sink.

4. A heat sink suitably tailored in space and time

The shortcomings of the uniform heat sink discussed in section 3 suggest how the postulated heat sink might be modified to give results closer to present day observation. First we note that the accumulated heat loss in each interval when the system reaches thermal equilibrium, characterized by the temperature distribution $T(z) = T_0 + z(T_1 - T_0)/L$, is proportional to $(1 - z/L)$. This suggests a heat sink varying linearly with $(1 - z/L)$. However given the same time scale as in section 3 this still produces a thermal boundary layer adjacent to the surface up to time t = 0.2 year, when the boundary layer and high surface heat flux disappear (see Figure 7). Most of the time there is a surface heat flux much larger than anything found on today's ocean floors except at hot spots on mid-ocean ridges. With a constant spreading rate (0.63 ms^{-1} as for the uniform heat sink) the shrinkage and depth profiles are the same as for the case of a uniform heat sink, i.e. linear.

In order to demonstrate the effect of the near-surface boundary layer we have increased the mesh resolution in this case to the finest available (Δz =47.5 m) and reduced the heat sink lifetime to 0.025 year (9.13 days) without changing the spreading rate. The resulting depth and surface heat flux profiles are shown in Figure 8. The close link between shrinkage and heat flux is obvious. Our predicted surface heat flux is clearly far too high. Further reducing the heat sink lifetime would not improve the match with observation; it would merely worsen the discrepancy between predicted and observed bathymetry.

This degree of mismatch between predicted and observed surface heat fluxes suggests a further modification of the shape of the postulated heat sink; it would seem that the heat sink must act much more strongly and quickly near the surface and at the earliest times. However a whole range of functional forms have been tried in our spreadsheets, and none have produced better fits to the data (i.e. the published heat flux and bathymetry curves in terms of uniformitarian time) than linear heat sink profiles of the form shown in equation (14); some forms (e.g. heat sink terms proportional to the square of the temperature disequilibrium) even produced heat flux curves with a minimum part way across the ocean basin.

Thus our 'final' (best estimate) version of a spreadsheet calculation

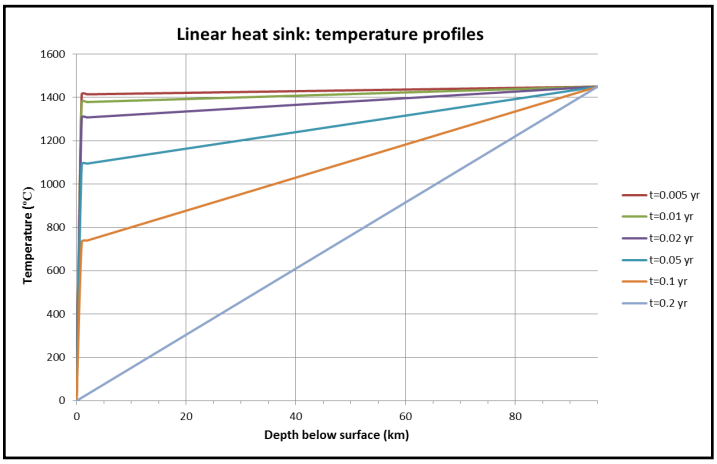

Figure 7. Temperature profiles in the case of a heat sink lasting for 0.2 year and varying linearly with depth, being zero at the bottom and maximum at the surface. Note the existence of a thermal boundary layer adjacent to the surface at all times prior to 0.2 year.

seeking to reproduce the data as closely as possible employs a heat sink of the form shown in equation (14). The input parameter values are $\Delta t = 0.0005$ year (~4.38 hours), $\tau_{hs} = 0.005$ year (~1.83 days), $\upsilon_0 = 0.22$ ms^{-1}, $\tau_f = 0.25$ year and $\tau_d = 0.2$ year (73 days). These values imply a maximum half spreading rate of 0.22 ms^{-1} and a total half-width of the ocean basin after 4,400 years of ~3,125 km (1,940 miles).

In order to minimize mesh resolution problems related to the near-surface thermal boundary layer, we have: (1) used the finest mesh resolution available; (2) modified the initial temperature profile to give an initial boundary layer thickness comparable with the mesh size. We did this by assuming a profile corresponding to the solution of the textbook half space problem after a notional 100 years. This stratagem has no time implications: it is used solely for computational convenience. Its implications are considered further in the Discussion section below. We have also (3) removed any formal inclusion of the thermal boundary layer in surface heat flux calculations, which are now done purely on the basis of temperature values stored on the mesh. This is done in order to remove the artificial kink in the heat flux curve which is otherwise observed as the boundary layer weakens and thickens over time until the flux it predicts falls below that based on mesh temperatures. Because of these changes we have run the calculations with three different mesh resolutions, viz. $\Delta z = 190$ m (i.e. 500 intervals through the plate), $\Delta z = 95$ m (1000 intervals) and $\Delta z = 47.5$ m (2000 intervals) and compared the results to check for mesh convergence. Although there are significant differences between these cases at early times, notably in the most sensitive output variable, viz. surface heat flux, they give very similar results for integrated quantities such as total heat loss and shrinkage. Table 2 lists the surface heat flux values for early times as output by the three calculations.

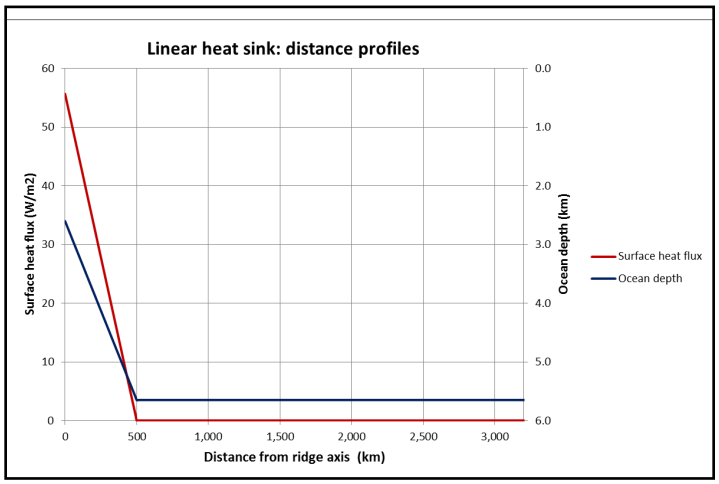

Figure 8. Plot of surface heat flux against distance from the ridge axis in the case of a heat sink varying linearly with depth (maximum at the surface, zero at the bottom of the plate) and lasting just 0.025 year (9.13 days), while the period of rapid spreading (0.63 ms^{-1}) lasts 0.2 year (73 days).

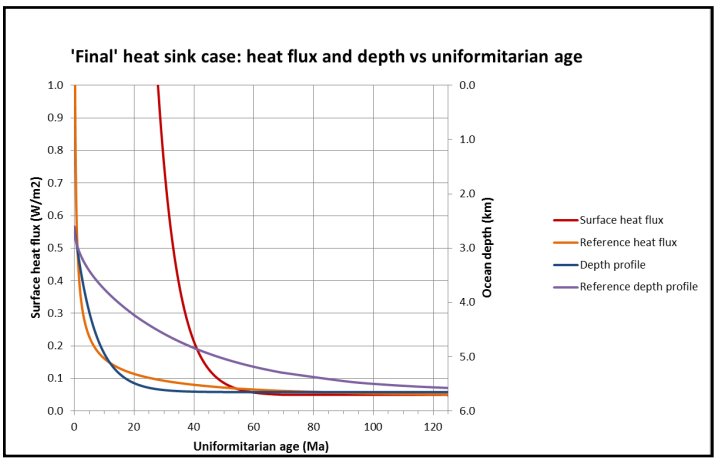

Figure 9. Plots of surface heat flux and ocean depth against equivalent uniformitarian age for our 'final' heat sink case. Reference curves based on the fitting equations given by Stein and Stein (1992) are included for comparison. The period of rapid spreading is 0.25 year (91.3 days), maximum speed 0.22 ms^{-1}.The results plotted here are based on the finest resolution mesh ($\Delta z = 47.5$ m). Note that the depth profile is too narrow while the heat flux is excessive across a significant fraction of the basin width.

Even in the most favourable case (defined by the input data given above) there are systematic conflicts with the observational data, most notably (1) the excessive surface heat fluxes seen at early times, i.e. in the central region of the ocean basin, and (2) the very rapid shrinkage seen close to the ridge; see Figure 9. The corresponding temperature profiles are shown in Figure 10. Although these features can be shifted by changing the time scales in the calculation, they are inevitably shifted together. For example, the calculated depth profile can be made fairly realistic by shrinking the spreading time scales to $\tau_f = 0.045$ year and $\tau_d = 0.09$ year while υ_0 is increased to 0.733 ms^{-1}. The results are plotted in Figure 11: while the depth profile is fairly realistic the surface heat flux is excessive over almost the whole width of the ocean basin.

DISCUSSION

1. Enhanced thermal conduction hypothesis

The physical properties of a material are determined by the locations of atoms within a crystal or molecule, the strength of the bonds between the atoms and the arrangement of the crystals or molecules. We are interested in thermal conductivity – the ability to transfer thermal energy by diffusion. Non-metals conduct thermal energy by the vibration of one atom causing its neighbour to vibrate and so on. The stronger the bond the more rapidly the energy is transferred, but a stronger bond also results in a stiffer crystal. The outstanding example is diamond, whose crystals are extremely stiff and conduct thermal energy almost as well as metals.

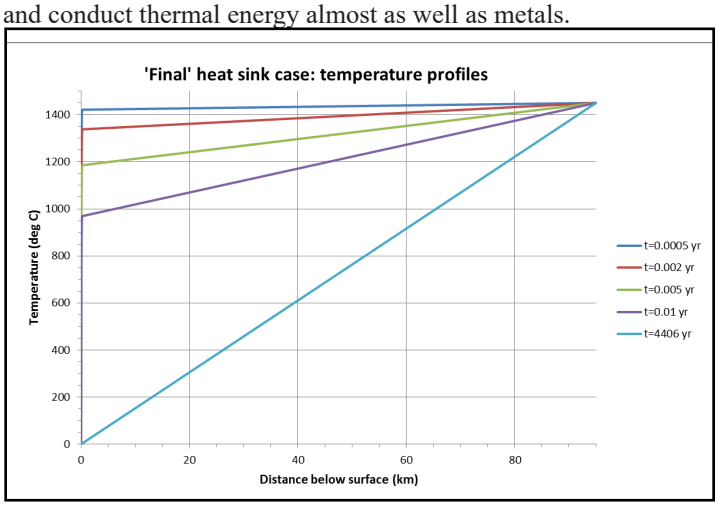

Figure 10. Temperature profiles for the final heat sink case ($\Delta z = 47.5$ m) in which the heat sink is proportional to the local temperature mismatch against the equilibrium state; at 4400 years the system is practically in equilibrium.

Metals are good conductors of both electricity and thermal energy because their structure de-localises or "frees" electrons to readily transport energy. The relevant point is that a change in a bulk property such as thermal conductivity is a consequence of changing the molecular structure, which will inevitably cause changes in other properties such as the thermal expansion coefficient, specific heat capacity and stiffness. In effect, one is creating a new material which may expand, heat up or respond to stress quite differently.

Drastically increasing lithospheric thermal conductivity would therefore inevitably cause changes, probably very large changes, in other material properties which we have kept constant in our calculations. Our "enhanced thermal conduction hypothesis" is therefore totally divorced from physical reality as well as demanding an extraordinary surface cooling mechanism. This use of multiple *ad hoc* hypotheses flies against the principle of Occam's razor, and we dismiss it as the least favoured of the rapid cooling options considered here.

2. Initial conditions in the simulations

For our final spreadsheet calculations ('Results' section, part 4) we have assumed a nonuniform temperature distribution at time $t = 0$ corresponding to the solution of the half space problem after 100 years. This is done in order to start with a thermal boundary layer with a thickness comparable to the mesh spacing, which in turn is intended to bring the calculation closer to mesh convergence than if we assumed a uniform initial temperature distribution. Although the 100 years of virtual 'prehistory' is arbitrary and cannot be justified on physical grounds, it does not significantly affect our results and certainly does not affect our main conclusions. In practice the magma rising to the surface will depressurise and cool as it does so, with one or more phase changes involving latent heat transfer and water release on the way. Given the rapidity of this process in a biblically-compatible time frame these changes are likely to be close to adiabatic. Since ocean water circulation within ocean floor basalts is important for present-day cooling, it is likely to have had even more impact during the Flood and immediate post-Flood periods. For these reasons the initial temperature profile will not be uniform. In order to run the calculations with more realistic initial conditions further investigation of the relevant literature and of the physical processes involved is needed.

3. The critical role of the thermal boundary layer

Apart from the enhanced conductivity case all the short time scale models we have considered are characterized by a near-surface thermal boundary layer at early times in the simulation. Such a boundary layer is inevitable on short time scales in a heat transfer problem in a poorly conducting medium with one boundary kept at a much lower temperature than the bulk, even in the presence of a strong heat sink. The key feature of a thermal boundary layer is that it is narrow and thus sustains a high conductive heat flux while the plate is shrinking rapidly because of the heat sink. This scenario appears unavoidable in the simple kind of plate model employed here.

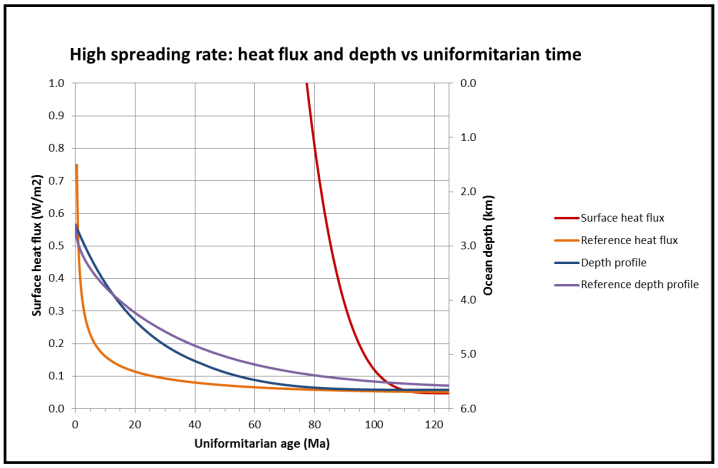

Figure 11. Illustrative plot equivalent to Figure 9 but assuming a shorter period of rapid motion, viz. 0.045 year (16.4 days) at 0.733 ms^{-1}. The approximate match with the reference depth profile is accompanied by an excessive heat flux across a very broad region.

4. Suggested further work

Even with several freely-chosen input parameters our simple plate models of ocean lithosphere formation within biblical time scales cannot reproduce key observational data. The main underlying problem is the presence of a near-surface thermal boundary layer. It is suggested that this modeling work should be developed further by using more realistic initial conditions and by incorporating several hitherto-neglected effects. These might include, for example, the heat removed by superheated water issuing from spreading centres (possibly corresponding to the 'fountains of the great deep', Genesis 7:11; cf. also Baumgardner 2003), phase changes and latent heat transfer during the rising and depressurizing of magma, production of water which stays within the cooling lithosphere, and hydrothermal flows. More sophisticated models accounting for these and possibly other effects may prove to be free of the problems encountered here.

CONCLUSION

There are some questions relating to origins, such as the origin of life, for which naturalistic scientists cannot produce satisfactory explanations. Ocean-floor cooling is the opposite: in the process of testing that our mathematical tools are fit for the purpose of modeling, we have confirmed that the long-age models are self-consistent, and agree with observations within an acceptable margin. The challenge is to produce a model consistent with observations and a biblical time scale.

We have demonstrated that this cannot easily be done on the hypothesis of removing heat from freshly-generated lithosphere over a period of less than a year. The underlying general reason for this is that at early times there is an inevitable near-surface thermal boundary layer which gives rise to high surface heat fluxes, even in the presence of a strong heat sink. Such boundary layers might potentially be avoided if more realistic initial conditions were used and hitherto missing geophysical effects included in our models.

ACKNOWLEDGEMENTS

Paul Garner assisted by providing access to some of the background literature cited here.

REFERENCES

Austin, S.A., J.R. Baumgardner, D.R. Humphreys, A.A. Snelling, L. Vardiman and K.P. Wise. 1994. Catastrophic Plate Tectonics: A Global Flood Model of Earth History. In *Proceedings of the Third International Conference on Creationism*, ed. R. E. Walsh, pp. 609–621. Pittsburgh, Pennsylvania: Creation Science Fellowship.

Barnes, R.O. 1980. Thermal consequences of a short time scale for sea-floor spreading, *JASA* 32:123-125.

Baumgardner, J.R. 2003. Catastrophic Plate Tectonics: The Physics Behind The Genesis Flood. In *Proceedings of the Fifth International Conference on Creationism*, ed. R. L. Ivey Jr., pp. 113–126. Pittsburgh, Pennsylvania: Creation Science Fellowship.

Bender, C.M. and S.A. Orszag. 1978. *Advanced Mathematical Methods for Scientists and Engineers.* McGraw-Hill Book Company.

Cramer, B.S., J.R. Toggweiler, J.D. Wright, M.E. Katz and K.G. Miller. 2009. Ocean overturning since the Late Cretaceous: Inferences from a new benthic foraminiferal isotope compilation, *Paleoceanography* 24, PA4216 (14 pages) [doi: 10.1029/2008PA001683].

Crosby, A.G., D. McKenzie and J.G. Sclater. 2006. The relationship between depth, age and gravity in the oceans, *Geophysical Journal International* 166:553-573 [doi: 10.1111/j.1365-246X.2006.03015.x].

Davies, J.H. and D.R. Davies. 2010. Earth's surface heat flux, *Solid Earth* 1:5-24.

Furlong, K.P. and D.S. Chapman. 2013. Heat flow, heat generation, and the thermal state of the lithosphere, *Annual Review of Earth and Planetary Sciences* 41:385–410.

Humphreys, D.R. 2000. Accelerated Nuclear Decay: A Viable Hypothesis? In *Radioisotopes and the Age of the Earth (Volume 1), A Young-Earth Creationist Research Initiative*, eds. L. Vardiman, A.A. Snelling and E.F. Chaffin, pp.333-379. Institute for Creation Research, El Cajon, California and Creation Research Society, St Joseph, Missouri.

Humphreys, D.R. 2005. Young Helium Diffusion Age of Zircons Supports Accelerated Nuclear Decay. In *Radioisotopes and the Age of the Earth (Volume 2), Results of a Young-Earth Creationist Research Initiative*, eds. L. Vardiman, A.A. Snelling and E.F. Chaffin, pp.25-100. Institute for Creation Research, El Cajon, California and Creation Research Society, Chino Valley, Arizona.

Lapidus, L. and G.F. Pinder. 1982. *Numerical Solution of Partial Differential Equations in Science and Engineering.* John Wiley & Sons, Inc.

McKenzie, D., J. Jackson and K. Priestley. 2005. Thermal structure of oceanic and continental lithosphere, *Earth and Planetary Science Letters* 233:337-349 [doi:10.1016/j.epsl.2005.02.005].

Mudelsee, M., T. Bickert, C.H. Lear and G. Lohmann. 2014. Cenozoic climate changes: A review based on time series analysis of marine benthic $\delta^{18}O$ records, *Reviews of Geophysics* 52, no. 3:333-374 [doi: 10.1002/2013RG000440].

Müller, R.D., M. Sdrolias, C. Gaina and W.R. Roest. 2008. Age, spreading rates, and spreading asymmetry of the world's ocean crust, *Geochemistry, Geophysics, Geosystems* 9, no. 4:1-19, Q04006 [doi: 10.1029/2007GC001743].

Parsons, B. and J.G. Sclater. 1977. An analysis of the variation of ocean floor bathymetry and heat flow with age, *Journal of Geophysical Research* 82, no. 5:803-827.

Qiuming, C. 2016. Fractal density and singularity analysis of heat flow over ocean ridges, *Scientific Reports* 6:19167 (pp.1-10) [doi: 10.1038/srep19167].

Seton, M., R.D. Müller, S. Zahirovic, C. Gaina, T. Torsvik, G. Shephard, A. Talsma, M. Gurnis, M. Turner, S. Maus and M. Chandler. 2012. Global continental and ocean basin reconstructions since 200 Ma, *Earth Science Reviews* 113:212-270.

Stein, C.A. and S. Stein. 1992. A model for the global variation in oceanic depth and heat flow with lithospheric age, *Nature* 359:123-129.

Turcotte, D.L. and G. Schubert. 2002. *Geodynamics (Second Edition)*. Cambridge University Press.

Vardiman, L., S.A. Austin, J.R. Baumgardner, S.W. Boyd, E.F. Chaffin, D.B. DeYoung, D.R. Humphreys and A.A. Snelling. 2005. Summary of Evidence for a Young Earth from the RATE Project. In *Radioisotopes and the Age of the Earth (Volume 2), Results of a Young-Earth Creationist Research Initiative*, eds. L. Vardiman, A.A. Snelling and E.F. Chaffin, pp.735-772. Institute for Creation Research, El Cajon, California and Creation Research Society, Chino Valley, Arizona.

Whittaker, J.M., A. Goncharov, S.E. Williams, R.D. Müller and G. Leitchenkov. 2013. Global sediment thickness data set updated for the Australian-Antarctic Southern Ocean, *Geochemistry, Geophysics, Geosystems* 14, no. 8:3297-3305 [doi: 10.1002/ggge.20181]. Associated global sediment thickness map entitled "Total Sediment Thickness of the World's Oceans and Marginal Seas, Version 2" can be found at https://www.ngdc.noaa.gov/mgg/sedthick/ (accessed 12th October 2017).

Zachos, J., M. Pagani, L. Sloan, E. Thomas and K. Billups. 2001. Trends, Rhythms and Aberrations in Global Climate 65 Ma to Present, *Science* 292:686-693.

NOMENCLATURE

adiabatic: An adiabatic process is one that occurs without transfer of heat or matter between a thermodynamic system and its surroundings.

bathymetry: The study of the depth of water in oceans, lakes or rivers; underwater topography.

half spreading rate: If two tectonic plates are separating from each other by (say) 20 mm per year, the half spreading rate for each plate is 10 mm/year. If they are spreading asymmetrically their half spreading rates will differ but still sum to 20 mm per year.

lithosphere: The mechanically distinct outer layer of the earth, consisting of the crust and the uppermost mantle, typically 50-100 km thick under the oceans and 100-300 km thick under the continents. It is distinctly cooler and more rigid than the asthenosphere, the relatively fluid, hot layer immediately below. The earth's tectonic plates consist of lithosphere.

THE AUTHORS

William J. Worraker is a part-time Research Associate with Biblical Creation Trust in the UK. He was employed as a computational physicist at AWE, Aldermaston, UK until retiring in March 2017. He has a BSc (Hons) in Physics from Bristol University, and a PhD, also from Bristol University, in fluid instability modeling. He has been an active amateur astronomer for over 25 years and has participated in collaborative professional-amateur observing projects and in writing the resulting peer-reviewed publications. He has written articles on astronomy and astrophysics in *Journal of Creation*, and a booklet entitled *Water in the Cosmos* published by Genesis Agendum in 2006. He gave two presentations at Origins 2016, the annual conference of the Creation Biology and Creation Geology Societies.

Richard Ward graduated in 1969 from Sidney Sussex College, Cambridge, where he studied mathematics and physics. After training at Leicester University he spent most of his life teaching physics to boys at Bishop Wordsworth's School, Salisbury, UK. Since retiring from teaching he has provided technical support at two schools, and has authored six articles published in the Institute of Physics (UK) journal Physics Education.